ChemPubSoc Europe

DOI: 10.1002/open.201500110

Open Access ChemistryOPEN Full Papers

Alcohol-Selective Oxidation in Water under Mild Conditions via a Novel Approach to Hybrid Composite Photocatalysts

Ali Abd-Elaal,[a, b, c] Francesco Parrino,*[b] Rosaria Ciriminna,[c] Vittorio Loddo,[b] Leonardo Palmisano,*[b] and Mario Pagliaro*[c]

This article is dedicated with affection to Prof. Laura M. Ilharco (Instituto Superior Técnico, Lisboa) on the occasion of the first decade of rewarding cooperation.

The oxidation of alcohols to carbonyl compounds in a clean fashion (i.e., with water as a solvent or under solvent-free conditions, and using O_2 or H_2O_2 as the primary oxidant) is the subject of considerable research efforts. A new approach for the selective oxidation of soluble aromatic alcohols in water under mild conditions via a novel composite photocatalyst has been developed. The catalyst is synthesized by grafting 4-(4-(4-hydroxyphenylimino)cyclohexa-2,5dienylideneamino)phenol and silver nanoparticles onto the surface of moderately crystalline titanium dioxide. The titanium dioxide-based composite was first extensively characterized and then employed in the catalytic oxidation of 4-methoxybenzyl alcohol to 4-methoxybenzaldehyde under UV irradiation in water at room temperature. The corresponding aldehyde was obtained with unprecedented high selectivity (up to 86%). The method is general and opens the route to fabrication of photocatalytic composites based on titanium dioxide functionalized with shuttle organic molecules and metal nanoparticles for a variety of oxidative conversions.

Introduction

The clean oxidation of alcohols to carbonyl compounds using no solvent or water as the reaction medium and oxygen or hydrogen peroxide as the primary oxidant is an important objective of contemporary chemical research.[1] The development of highly desirable selective photocatalytic processes using visible light or ultraviolet (UV) photons and oxygen as reactants at room temperature, in particular, is the object of considerable research efforts,[2] with examples ranging from the selective oxidation of glycerol over sol-gel-encapsulated bismuth tungstate (Bi_2WO_6),[3] to sulfoxidation of alkanes,[4] conversion of ferulic acid into vanillin,[5] and of alcohols into aldehydes.[6]

Even though generally requiring energetic UV radiation, the use of cheap titanium dioxide as a photocatalyst for organic synthesis is of relevant practical interest due to its abundance, nontoxic nature and pronounced stability.[2] In general, the presence of water enhances the unselective mineralization activity of nanostructured titanium dioxide.[7] Titanium dioxide possessing moderate crystallinity shows higher selectivity. On the other hand, the highly ordered crystal lattice of titanium dioxide, especially in the anatase form, makes the mineralization path faster than the adsorption/desorption steps, so that the target products are mineralized before being desorbed.[8] For this reason, although high selectivity (> 99%) towards aldehyde for alcohol oxidation conducted in harmful solvents, such as acetonitrile[9] or trifluoromethylbenzene,[10] or in the presence of different catalysts has been reported,[11] the achievement of high selectivity in processes carried out in aqueous systems and in the presence of titanium dioxide is still a challenge.

One elegant and effective approach to enhance selectivity relies on increasing the affinity between the target reactant and the catalyst surface. For instance, the hydrophobicity of the catalyst can be opportunely tuned by grafting the surface of P25 titania (commercial TiO_2 composed of 80% anatase and 20% rutile with a specific surface area of 50 $m^2 g^{-1}$) with *n*-octyl groups, affording a material that exhibits good selectivity when employed for the selective oxidation of nonylphenol.[12]

[a] *Dr. A. Abd-Elaal[+]*
Egyptian Petroleum Research Institute
1 Ahmed El-Zomor St., 11727 Cairo (Egypt)

[b] *Dr. A. Abd-Elaal,[+] Dr. F. Parrino,[+] Prof. V. Loddo, Prof. L. Palmisano*
"Schiavello-Grillone" Photocatalysis Group, DEIM
Università degli Studi di Palermo
viale delle Scienze, 90128 Palermo (Italy)
E-mail: francesco.parrino@unipa.it
leonardo.palmisano@unipa.it

[c] *Dr. A. Abd-Elaal,[+] Dr. R. Ciriminna, Prof. M. Pagliaro*
Istituto per lo Studio dei Materiali Nanostrutturati, CNR
Via U. La Malfa, 153-90146 Palermo (Italy)
E-mail: mario.pagliaro@cnr.it

[+] *These authors contributed equally to this paper.*

Supporting information for this article is available on the WWW under http://dx.doi.org/10.1002/open.201500110.

In another approach, the selectivity is enhanced by decreasing the residence time of the reaction product, thereby preventing further oxidation as demonstrated with aromatic alcohols to the corresponding aldehydes.[13] Finally, doping of titanium dioxide with metal nanoparticles (NPs) has also been effectively used as a strategy for enhancing selectivity, such as in the case of gold NPs deposited at the anatase–rutile interface for the partial oxidation of alcohols to the corresponding aldehydes,[14] as well as for P25 titania loaded with iridium and palladium nanoclusters.[15]

In this work, we describe a novel approach to the selective photocatalytic oxidation of 4-methoxybenzyl alcohol (4-MBA) to 4-methoxybenzaldehyde (4-MBD) in water using a hybrid titanium dioxide-based photocatalyst functionalized with conjugate organic molecule 4-(4-(4-hydroxyphenylimino)cyclohexa-2,5dienylideneamino)phenol (DIOL), easily synthesized via condensation of *p*-quinone and 4-aminophenol (Scheme 1), and silver NPs. The method is general, and the observed selectivity towards the aldehyde of up to 86% is, to the best of our knowledge, the highest reported for reactions in water suspensions of titanium dioxide thus far.

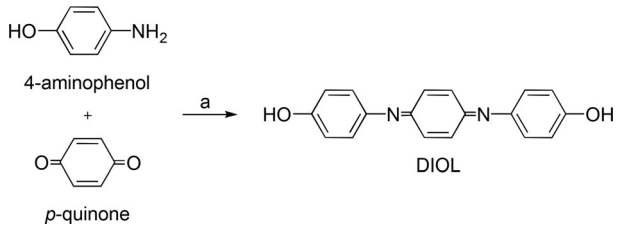

Scheme 1. Synthesis of DIOL. *Reagents and conditions*: a) EtOH, reflux, 6 h.

Results and Discussion

Two laboratory-prepared titanium dioxide catalysts, HP1 (mixture of anatase and rutile phases) and Rutile (rutile phase only), were functionalized with DIOL and silver NPs and employed in the oxidation of 4-MBA in water. The materials were opportunely designed in order to obtain photocatalysts able to fulfill most of the requirements necessary to achieve high selectivity in the partial oxidation of aromatic alcohols to aldehydes.

HP1 and Rutile were chosen as the basis for the catalysts because of their poor crystallinity degree. In fact, it is known that high activity arising from the highly ordered crystal lattice of titanium dioxide makes the mineralization path faster than the adsorption/desorption steps, so that the target products are mineralized before being desorbed.[8] DIOL was opportunely synthesized in order to facilitate adsorption of the aromatic alcohol and to allow fast interfacial electron transfer due to its high conjugation. Table 1 shows the highest selectivity values towards 4-MBD. For comparison, the unfunctionalized titanium dioxide materials were tested in the same reaction.

Both HP1 and Rutile samples were active (Entries 1 and 5; Table 1), with Rutile being more selective. Functionalization of HP1 with DIOL increases the selectivity from 39 to 48.5% (Entry 3; Table 1), while the presence of both DIOL and silver NPs results in selectivity that is twice as high with respect to both unfunctionalized HP1 and Rutile (Entries 4 and 8, respectively; Table 1).

Table 1. Irradiation time (t_{irr}), 4-methoxybenzyl alcohol (4-MBA) conversion (%) and highest selectivity (%) towards 4-methoxybenzaldehyde (4-MBD) reached for partial oxidation of 4-MBA in the presence of different photocatalysts (0.2 g L^{-1}), at natural pH, in the presence of air and under UV irradiation.

Entry	Photocatalyst[a]	t_{irr} [min]	Conversion [%]	Selectivity [%]
1	HP1	180	38.0	39.0
2	HP1-S	200	37.0	36.0
3	HP1-D	840	34.0	48.5
4	HP1-D-S	300	25.0	70.0
5	Rutile	360	60.0	43.0
6	Rutile-S	360	62.0	39.0
7	Rutile-D	360	39.0	62.0
8	Rutile-D-S	360	54.0	86.0

[a] Laboratory-prepared titanium dioxide catalysts: HP1 (anatase/rutile) and Rutile (pure rutile) functionalized with DIOL (D) and/or Ag NPs (S).

In order to check the influence of silver NPs without the concurrent presence of DIOL, the same reaction was carried out using silver NPs-functionalized HP1 (HP1-S) and Rutile (Rutile-S) (Entries 2 and 6; Table 1). In both cases, the values of conversion and maximum selectivity toward 4-MBD were similar to those obtained in the presence of the corresponding unfunctionalized samples, indicating that the effect of silver NPs in increasing selectivity is strongly bound to the presence of DIOL.

Figure 1 shows the kinetics of 4-MBA photocatalytic oxidation run in water in the presence of Rutile-D-S (Rutile functionalized with both diol and silver NPs) at room temperature. The major oxidation product was 4-MBD, along with CO_2. All the reactivity runs indicated that the rate of formation of aldehyde and CO_2 is different from zero from the beginning of irradiation, thus suggesting that their formation starts in concomitance with irradiation.

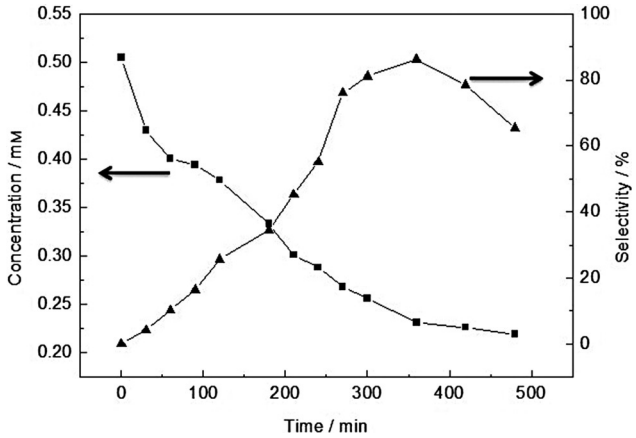

Figure 1. 4-MBA concentration (■) and selectivity towards 4-MBD (▲) versus irradiation time (t_{irr}). Photocatalyst: Rutile-D-S (0.2 g L^{-1}).

Prolonging the reaction time results in mineralization of the reaction product as well as the formation of traces of 4-methoxybenzoic acid. Indeed, for all catalysts studied, the selectivity in each run increased until a maximum, and then decreased at higher irradiation times. This typical trend can be explained by considering that the selectivity towards 4-MBD increases until its concentration in the liquid phase limits the desorption from the catalyst surface, so that its degradation becomes relevant.

Blank experiments carried out under visible light (using a 100 W tungsten halogen lamp with emitted radiation at $\lambda \leq 400$ nm cut off by means of a 1 M $NaNO_2$ solution) showed negligible conversion of 4-MBA, indicating that UV light irradiation is necessary for this reaction.

The stability of the DIOL molecule adsorbed onto the surface of titanium dioxide was proved by irradiating a water suspension of HP1-D catalyst (functionalized with DIOL only) under UV light for 20 h. Samples were taken at fixed time intervals and analyzed by means of a total organic carbon (TOC) analyzer. The amount of dissolved organic carbon was negligible for all samples, showing the stability of the composite.

To check catalyst reusability, after the partial oxidation run, the HP1-D catalyst was carefully washed and reused for another run. Almost the same activity and selectivity were obtained in the two sequential tests, confirming the reusability and stability of the catalyst. Similar tests were carried out using HP1-D-S and Rutile-D-S. Also in this case, the stability of DIOL was confirmed. Moreover, the amount of silver released in solution was qualitatively monitored by adding chloride ions. The amount of silver chloride thus produced was negligible in all samples withdrawn during each run.

The enhancement in selectivity of the modified catalyst can be ascribed both to the increased adsorption of the aromatic alcohol at the titanium dioxide surface modified with phenol groups, and to the decreased affinity for the surface of the aromatic aldehyde. In fact, once formed, the aromatic aldehyde, with lower chemical affinity for the irradiated surface compared with alcohol or water, would easily desorb avoiding further oxidation. Furthermore, the conjugated structure of the DIOL molecule allows fast electron transfer from the titanium dioxide to the outer shell of the composite where the redox reaction occurs.

The role of the silver NPs in further increasing both the selectivity and conversion of the reaction is due to the effective electronic junction between titanium dioxide and silver. DIOL acts as a molecular conductive bridge between them. As a consequence a better spatial charge separation is achieved.

The Ti–O bond between titanium dioxide and DIOL has been reported as the preferential interaction for phenolic species adsorbed on titanium dioxide.[16] The majority of silver NPs deposited on the DIOL-grafted titanium dioxide are likely covalently attached to the terminal phenolic oxygen of DIOL (Figure 2); however, a direct interaction of Ag NPs with the titanium dioxide surface cannot be ruled out.[17]

Figure 3 shows the temporal trend of 4-MBA concentration for runs in the presence of Rutile, Rutile-D and Rutile-D-S catalysts (a similar trend, not shown, was observed also in the case of HP1 catalysts). The presence of DIOL molecules on the surface of the titanium dioxide strongly depresses the activity with respect to unfunctionalized titanium dioxide. However, the activity of Rutile-D-S was higher than that observed for the Rutile-D sample, again due to the photogenerated electrons conveyed by the metal NPs and to the subsequent lower electron-hole recombination and higher radical production.

The scanning electron microscope (SEM) images of HP1 and of Rutile samples in Figure 4 show that all catalyst samples are comprised of aggregated spherical particles with diameter ranging from 40 to 70 nm. In the case of HP1, the presence of DIOL molecules during the preparation procedure causes the

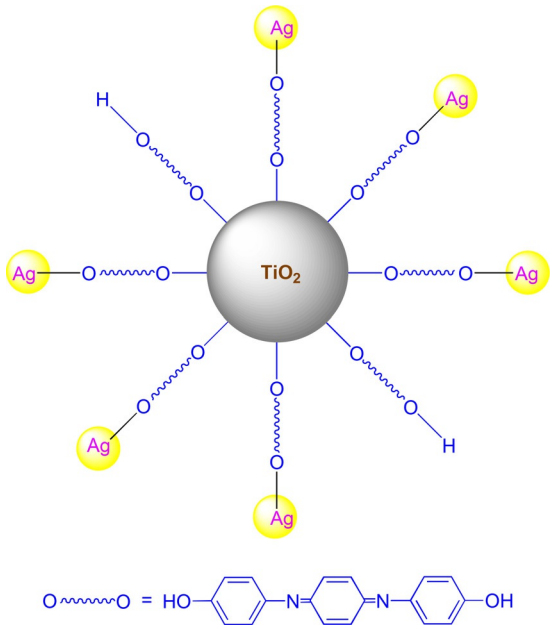

Figure 2. Representation of the TiO_2/DIOL/Ag composite structure. For clarity, only one possible adsorption mode of DIOL onto the TiO_2 surface is shown; however, adsorption via π–π interaction of the benzene rings or through the nitrogen lone pair cannot be ruled out.

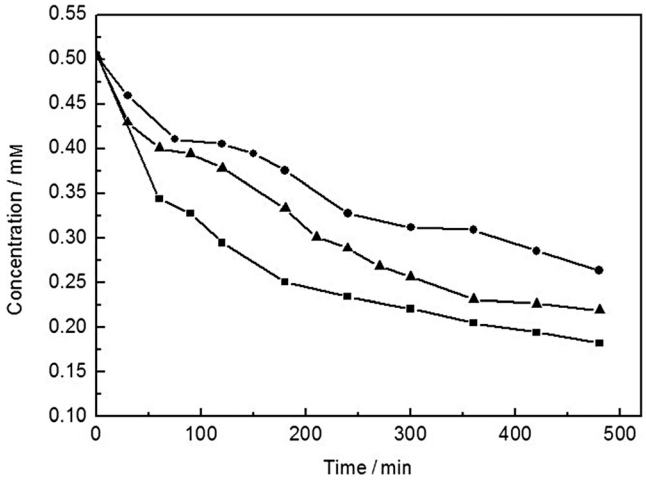

Figure 3. 4-MBA concentration versus irradiation time (t_{irr}) for runs carried out in the presence of Rutile (■), Rutile-D (●) and Rutile-D-S (▲).

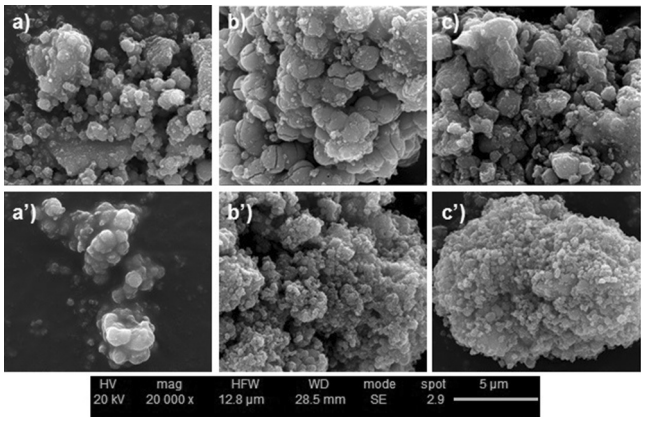

Figure 4. Scanning electron microscopy (SEM) images of HP1 (a), HP1-D (b), HP1-D-S (c), Rutile (a'), Rutile-D (b'), Rutile-D-S (c').

formation of larger spherical agglomerates, with diameters of about 1.5 µm. Energy-dispersive X-ray analysis (EDAX) confirmed the presence of silver both in HP1-D-S and in Rutile-D-S samples. For both samples the silver weight percentage was 2.3%.

The UV-vis absorption profiles of the investigated catalysts are shown in Figure 5. The unfunctionalized titanium dioxide samples show an absorption edge at 400 nm, corresponding to electron excitation from the conduction to the valence band.

The presence of DIOL in samples HP1-D and Rutile-D introduces a novel broad absorption in the visible region of the spectra. Two bands roughly centered at 450 and 600 nm are also evident (especially for the Rutile-D and Rutile-D-S) in the absorbance spectrum of pure DIOL (Figure 6). The broad absorption up to 800 nm explains the grey color of the DIOL containing powders. The presence of silver NPs does not produce any change in the optical behavior of the powders, likely due to the intense DIOL absorption in the visible region.

The reduction and oxidation potentials of DIOL were calculated by means of cyclic voltammetry from the mediated anodic and cathodic peak potentials as the shape of the curves shows the presence of reversible electron-transfer processes. The values were confidently correlated to the highest occupied molecular orbital (HOMO) and to the lowest unoccupied molecular orbital (LUMO), since the experiments were carried out in the absence of oxygen and water in order to avoid degradation of the organic species.

The relationships described by Equations (1) and (2) were applied according to the relevant literature,[6,18] where $E_{Ag/Ag+}$ is the potential of Ag/Ag^+ versus normal hydrogen electrode (NHE) (0.36 V).

$$E_{LUMO} = [-(E_{red1/2} + E_{Ag/Ag^+}) - 4.5]\ \text{eV} \quad (1)$$

$$E_{HOMO} = [-(E_{ox1/2} + E_{Ag/Ag^+}) - 4.5]\ \text{eV} \quad (2)$$

Based on the cyclic voltammetry results (Supporting Information), the HOMO and LUMO of DIOL were determined to be −5.3 and −3.6 eV, respectively, so that the energy gap of DIOL is aproximately 1.7 eV. This energy gap corresponds to a wavelength of about 1240/1.7 = 730 nm, a value in good agreement with the absorption onset shown in the absorbance spectrum of DIOL in ethanol (Figure 6).

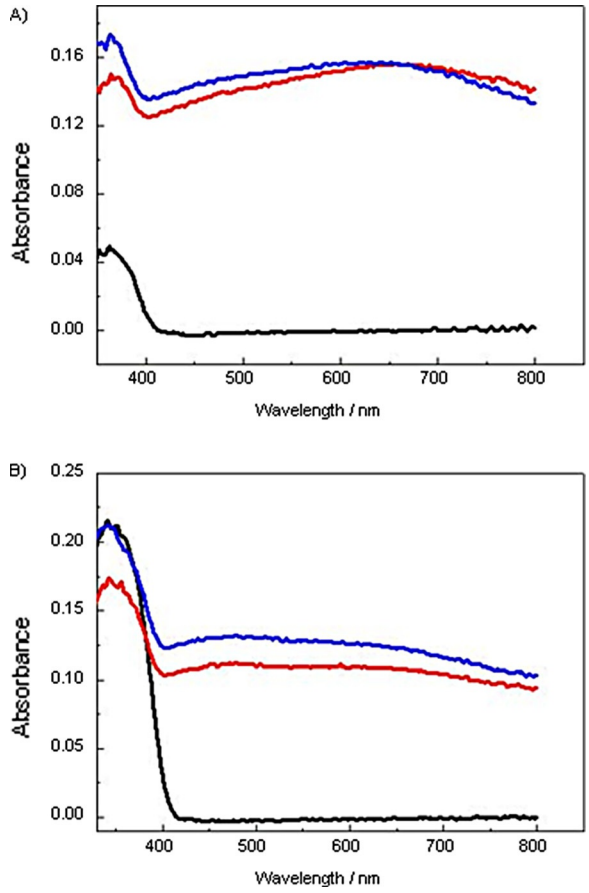

Figure 5. Diffuse reflectance spectra of A) Rutile (——), Rutile-D (——), Rutile-D-S (—— and B) HP1 (——), HP1-D (——), HP1-D-S (——).

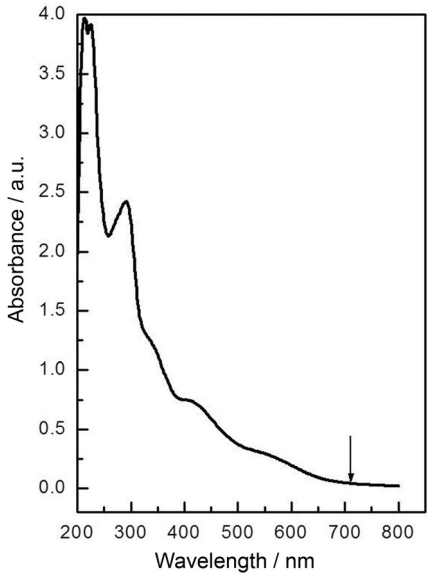

Figure 6. Absorbance spectrum of DIOL in ethanol.

The X-ray powder diffraction (XRD) patterns in Figure 7 of the HP1 catalyst series show that they are comprised of a mixture of anatase and rutile phases, whereas the patterns of the Rutile catalyst series show that the materials present the pure rutile phase. The presence of an amorphous phase also cannot be excluded. As far as the HP1 samples are concerned, it is evident that the presence of DIOL during the material synthesis decreases the formation of the anatase phase.

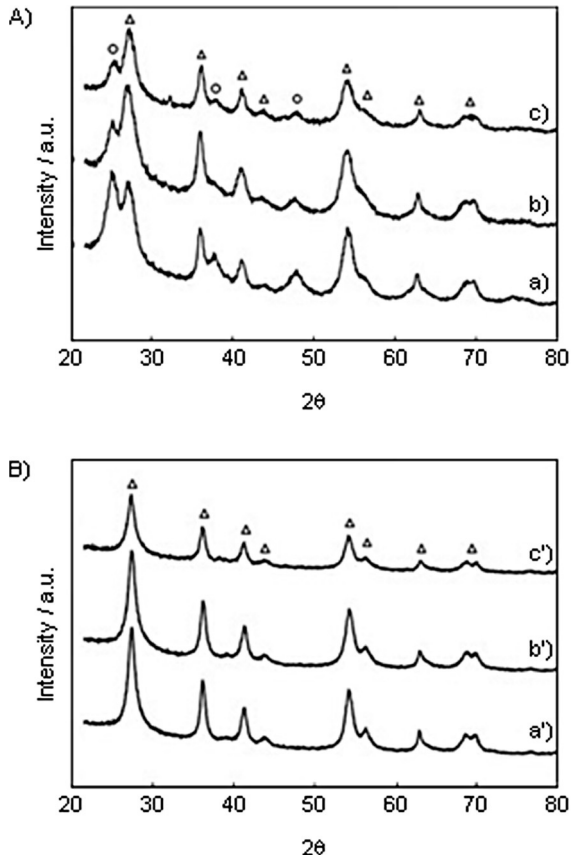

Figure 7. X-ray powder diffraction (XRD) patterns of A) HP1 (a), HP1-D (b), HP1-D-S (c), and B) Rutile (a′), Rutile-D (b′) and Rutile-D-S (c′). Symbols indicate anatase (○) and rutile (△) patterns.

From the cyclic voltammetry data obtained from a solution of DIOL in acetonitrile and from the electronic structure of HP1 and Rutile,[19] it is possible to draw a mechanistic scheme of the electronic transitions in the HP1-D and Rutile-D catalysts (Scheme 2). The relative position of the energy levels explains the stability of the composite *and* the absence of dissolved organic carbon of a water suspension of HP1-D under UV irradiation.

Under UV irradiation, both HP1 and DIOL absorb the UV photons. However, the DIOL molecule cannot be oxidized by the holes photogenerated in the valence band of titanium dioxide (oxidation thermodynamically not favored). Similar considerations can be also made for the Rutile-D sample. Indeed, although in this case the energy of the conduction band of Rutile results about 0.2 eV lower than that of HP1, the relative positions of the energetic levels is retained. Once generated

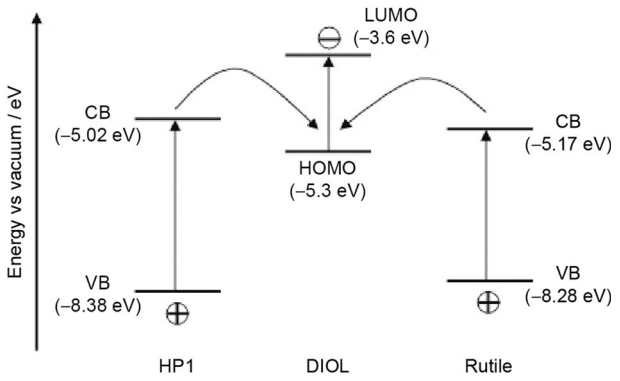

Scheme 2. Mechanistic scheme of electronic transitions of HP1-D and Rutile-D under UV irradiation.

and spatially separated, electrons and holes initiate the well-known photocatalytic mechanism described in the relevant literature[6,9,13,19,20] for aldehyde formation.

Conclusions

We have used an integrated approach to develop a composite hybrid material made of titanium dioxide functionalized with an organic conjugated phenol (DIOL) and silver NPs suitable for the selective oxidation of water soluble aromatic alcohols to aldehydes in water under UV irradiation and very mild conditions.

The 86% selectivity observed for the Rutile/DIOL/Ag composite is, to the best of our knowledge, the highest thus far reported for partial oxidation of aromatic alcohols to aldehydes in water suspensions of titanium dioxide.

The method is general as it relies on the concomitant easier adsorption of the aromatic alcohol and more facile release of the aldehyde, coupled to fast interfacial electron transfer due to the conjugated DIOL acting as a molecular electron bridge covalently bound to both silver NPs and titanium dioxide.

Modification of the shuttle molecule as well as utilization of other metal NPs could potentially open the route to optimization of the selective conversion for several other photocatalytic redox reactions mediated by similar advanced titanium dioxide-based composites.

Experimental Section

Syntheses and catalyst preparation

All chemicals were purchased from Sigma–Aldrich and used as received without any further purification.

Synthesis of DIOL: The synthesis was carried out following a previously reported procedure for Schiff base reaction.[21] *p*-Quinone (10.81 g, 0.1 mol) was condensed with *p*-aminophenol (21.82 g, 0.2 mol) in the presence of EtOH (100 mL) as a solvent. The reaction mixture was heated at reflux for 6 h and then left to stand overnight until the product precipitated. The product was isolated by filtration, washed with petroleum ether, and then recrystallized from EtOH and dried under vacuum at 313 K.

Synthesis of Ag NPs: A chemical reduction method was used to prepare a colloidal solution of Ag NPs.[22–24] An aqueous solution of $AgNO_3$ (10^{-3} M, 100 mL) was heated until boiling. Then, an aqueous solution of trisodium citrate (10 mL, 1% *w/w*) was added dropwise. The resulting mixture was vigorously stirred and heated at about 373 K until the solution turned yellow. The resulting suspension was stirred while slowly cooling to room temperature.

Catalysts preparation: The preparation of Rutile and HP1 catalysts was reported elsewhere.[13,19] The catalysts functionalized with DIOL (HP1-D and Rutile-D) were prepared similarly to the corresponding pure TiO_2 samples, but the $TiCl_4$ hydrolysis step was carried out in the presence of DIOL. In particular, for the HP1-D sample, $TiCl_4$ (1.12 mL, 0.01 mol) was added dropwise to an aqueous solution of DIOL (58 mg, 0.2 mmol). The mixture was stirred overnight at room temperature and then heated at reflux for 1 h. After cooling, the precipitate was isolated by filtration, washed several times with distilled water to eliminate the physically adsorbed DIOL, and dried overnight at 323 K.

The Rutile-D sample was prepared by adding $TiCl_4$ (20 mL, 0.18 mol) to an aqueous solution of DIOL (450 mg in 1000 mL). Both HP1-D and Rutile-D samples appeared as grey powders.

HP1-D-S and Rutile-D-S were synthesized by stirring DIOL-only functionalized material (0.4 g) with an Ag NPs suspension (25 mL), prepared as described above, overnight at room temperature. The suspension was then centrifuged, and the powder was washed five times to eliminate the non-bound Ag NPs. The materials was then dried overnight at 323 K. For comparison purposes, the HP1-S sample was prepared by stirring HP1 (0.4 g) in a colloidal suspension of Ag NPs (25 mL) overnight at room temperature. The material was isolated by filtration, and the powder was washed five times with distilled water and dried overnight at 323 K.

DIOL and catalyst characterization

The structure of the synthesized DIOL was confirmed by means of Fourier transform infrared (FTIR) and ^{1}H NMR spectroscopies. The IR analysis was performed by using a FTIR 8400 Shimadzu spectrophotometer. The ^{1}H NMR spectrum was recorded at 200 MHz in [D_6]DMSO, using a Brucker AC-E series 200 MHz spectrometer (NMR data are in the Supporting Information). The HOMO and LUMO of the DIOL were determined by means of cyclic voltammetry measurements, carried out in a three-electrode electrochemical cell by using a CH Instruments electrochemical analyzer. The reference electrode was a non-aqueous Ag/Ag^+ (0.01 M solution of [Bu_4N][ClO_4] in MeCN) provided by Amel Electrochemistry. The counter electrode was a platinum foil (surface area equal to ca. 0.5 cm^2). The working electrode was a fluorine-doped tin oxide (FTO)-functionalized glass electrode (Pilkington TEC15), which was previously washed with acetone and dried in air. The electrolytic solution was made of 0.1 M $LiClO_4$ in anhydrous MeCN with a fixed amount of DIOL dissolved in it.

Cyclic voltammetric measurements were taken at different ranges of potential, operating both in reduction and in oxidation modes, with a scan rate of 50 mV s^{-1}. Before each voltammetry, the electrolytic solution was stirred by a magnetic stirrer and bubbled with N_2 for 0.5 h to remove traces of O_2.

UV-vis spectra in the 200–800 nm range were obtained in absorbance mode for solutions and in reflectance mode for powders. A Shimadzu UV-2401 PC spectrophotometer was used, and the diffuse reflectance spectra (DRS) were recorded by mixing sample powder (50 mg) with $BaSO_4$ (2 g). The X-ray diffraction patterns were obtained by means of an analytical Empyrean diffractometer using the Cu Kα radiation with a Pixcel 1D detector. The morphology of the catalyst was examined using a Philips XL30 ESEM scanning electron microscope (SEM), operating at 30 kV on specimens upon which a thin layer of gold was deposited. Specific surface areas of HP1 and Rutile photocatalysts were measured by means of a FlowSorb 2300 apparatus (Micromeritics) by using the single-point Brunauer–Emmett–Teller (BET) method; values were determined to be 230 and 118 $m^2 g^{-1}$, respectively. Values for HP1-D and Rutile-D could not be determined due to thermal decomposition of DIOL during the degassing treatments (250 °C).

Photocatalytic setup and analytical techniques

The photocatalytic partial oxidation runs in liquid phase were carried out with an initial substrate concentration of 0.5 mM by using a cylindrical photoreactor (CPR; internal diameter: 32 mm, height: 188 mm) containing an aqueous suspension of the photocatalyst (150 mL). The reaction mixture in the reactor was irradiated by three external Actinic BL TL MINI 15 W/10 Philips fluorescent lamps with a main emission peak in the near-UV region at 365 nm. The reactor was cooled by water circulating through a Pyrex thimble, so that the temperature of the suspension was about 300 K. The radiation intensity impinging on the suspension was measured by a radiometer Delta Ohm DO9721 with an UV-A probe; the radiation power absorbed per unit volume of suspension was about 0.76 mW mL^{-1}. The lamps were switched on at time (t) = 0, after 0.5 h of stirring the suspension in the dark.

The runs were performed in the presence of air. The catalyst concentration used was 0.2 g L^{-1}. The values of substrate concentration before the addition of catalyst and before starting the irradiation were measured in order to determine the substrate adsorption on the catalyst surface under dark conditions. During the reaction runs samples withdrawn at fixed times were immediately filtered through 0.25 or 0.45 μm membranes (HA, Millipore) before analyses. The quantitative determination of the starting molecules, and their oxidation products were performed by means of a Beckman Coulter HPLC (System Gold 126 solvent module and 168 diode array detector), equipped with a Phenomenex 150×4.60 mm Kinetex 5u C18 100A column at 298 K.

The eluent consisted of a mixture of MeCN and 1 mM aqueous trifluoroacetic acid solution (20:80 *v/v*). The flow rate was set at 0.6 mL min^{-1}. Retention times (t_R) and UV spectra of the compounds were compared with those of standards purchased from Sigma–Aldrich (99%). TOC analyses were carried out by a 5000 A Shimadzu analyzer.

Acknowledgements

The authors thank the Italian Ministry of Foreign Affairs for funding Dr. Ali Abd-Elaal's stay in Italy via a "Scienze per la DIPLOMazia: Multidisciplinary Training Programme" grant. The authors also thank Dr. Antonino Adamo and Mrs. Arianna Falco (CNR–IAMC Mazara del Vallo, Italy) for constant support to Dr. Abd-Elaal, and to the University of Palermo's Prof. Antonino Lauria (STEMBIO) and Dr. Bartolo Megna (DICAM) for NMR and X-ray powder diffraction analyses, respectively.

Keywords: alcohol oxidation · composites · nanostructures · photocatalysis · titanium dioxide

[1] R. A. Sheldon, *Catal. Today* **2015**, *247*, 4–13.
[2] G. Palmisano, V. Augugliaro, M. Pagliaro, L. Palmisano, *Chem. Commun.* **2007**, 3425–3437.
[3] Y. Zhang, R. Ciriminna, G. Palmisano, Y. Xu, M. Pagliaro, *RSC Adv.* **2014**, *4*, 18341–18346.
[4] F. Parrino, A. Ramakrishnan, C. Damm, H. Kisch, *ChemPlusChem* **2012**, *77*, 713–720.
[5] F. Parrino, V. Augugliaro, G. Camera-Roda, V. Loddo, M. J. López-Muñoz, C. Márquez-Álvarez, G. Palmisano, L. Palmisano, M. A. Puma, *J. Catal.* **2012**, *295*, 254–260.
[6] C. Guarisco, G. Palmisano, G. Calogero, R. Ciriminna, G. Di Marco, V. Loddo, M. Pagliaro, F. Parrino, *Environ. Sci. Pollut. Res. Int.* **2014**, *21*, 11135–11141.
[7] M. Bellardita, V. Loddo, A. Mele, W. Panzeri, F. Parrino, I. Pibiri, L. Palmisano, *RSC Adv.* **2014**, *4*, 40859–40864.
[8] M. A. Lazar, W. A. Daoud, *RSC Adv.* **2012**, *2*, 447–452.
[9] S. Higashimoto, N. Kitao, N. Yoshida, T. Sakura, M. Azuma, H. Ohue, Y. Sakata, *J. Catal.* **2009**, *266*, 279–285.
[10] S. Furukawa, T. Shishido, K. Teramura, T. Tanaka, *ChemPhysChem* **2014**, *15*, 2665–2667.
[11] A. Tanaka, K. Hashimoto, H. Kominami, *J. Am. Chem. Soc.* **2012**, *134*, 14526–14533.
[12] K. Inumaru, T. Kasahara, M. Yasui, S. Yamanaka, *Chem. Commun.* **2005**, 2131–2133.
[13] V. Augugliaro, H. Kisch, V. Loddo, M. J. López-Muñoz, C. Márquez-Álvarez, G. Palmisano, L. Palmisano, F. Parrino, S. Yurdakal, *Appl. Catal. A* **2008**, *349*, 182–188.
[14] D. Tsukamoto, Y. Shiraishi, Y. Sugano, S. Ichikawa, S. Tanaka, T. Hirai, *J. Am. Chem. Soc.* **2012**, *134*, 6309–6315.
[15] W. Feng, G. J. Wu, L. D. Li, N. J. Guan, *Green Chem.* **2011**, *13*, 3265–3272.
[16] S. Kim, W. Choi, *J. Phys. Chem. B* **2005**, *109*, 5143–5149.
[17] I. E. dell'Erba, C. E. Hoppe, R. J. J. Williams, *Langmuir* **2010**, *26*, 2042–2049.
[18] P. Deng, L. Liu, S. Ren, H. Li, Q. Zhang, *Chem. Commun.* **2012**, *48*, 6960–6962.
[19] V. Augugliaro, H. Kisch, V. Loddo, M. J. López-Muñoz, C. Márquez-Álvarez, G. Palmisano, L. Palmisano, F. Parrino, S. Yurdakal, *Appl. Catal. A* **2008**, *349*, 189–197. The conduction and valence band edges of HP1 catalyst are the same as the HP0.5, HP2, HP4 and HP6 samples reported in this reference. In fact, varying the boiling time from 0.5 to 6 h does not influence the electronic properties of the powders. The electronic features of the Rutile sample are assumed to be similar to those of the HP8 sample (pure rutile phase).
[20] S. Yurdakal, G. Palmisano, V. Loddo, O. Alagöz, V. Augugliaro, L. Palmisano, *Green Chem.* **2009**, *11*, 510–516.
[21] S. M. Shaban, A. Saied, S. M. Tawfik, A. Abd-Elaal, I. Aiad, *J. Ind. Eng. Chem.* **2013**, *19*, 2004–2009.
[22] M. S. Azzam, A. F. El-Frarrge, D. A. Ismail, A. Abd-Elaal, *J. Dispersion Sci. Technol.* **2011**, *32*, 816–821.
[23] N. A. Negm, S. M. Tawfik, A. Abd-Elaal, *J. Ind. Eng. Chem.* **2015**, *21*, 1051–1057.
[24] A. Abd-Elaal, S. M. Tawfik, S. M. Shaban, *Appl. Surf. Sci.* **2015**, *342*, 144–153.

Received: April 21, 2015
Published online on July 14, 2015

